

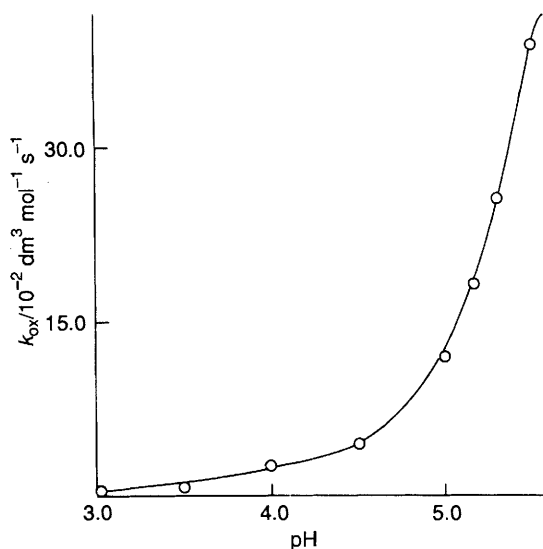
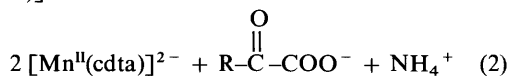
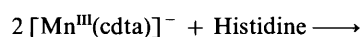
Table 1 Kinetic data for the reduction of $\text{Co}^{\text{III}}\text{W}$ by histidine with $[\text{Co}^{\text{III}}\text{W}] = 2.0 \times 10^{-4} \text{ mol dm}^{-3}$, $I = 1.0 \text{ mol dm}^{-3}$ (NaClO_4) at 60°C

[Hist]/ $10^{-1} \text{ mol dm}^{-3}$	$k_{\text{obs}}/10^{-3} \text{ s}^{-1}$	
	pH = 3.0	pH = 4.0
0.08	0.08	0.40
0.10	0.11	0.56
0.30	0.31	1.60
0.50	0.52	2.97
0.80	0.84	5.10

Table 2 Kinetic data for the reduction of $[\text{Mn}^{\text{III}}(\text{cdta})]^-$ by histidine with $[\text{Mn}^{\text{III}}(\text{cdta})]^- = 1.0 \times 10^{-3} \text{ mol dm}^{-3}$, $I = 0.50 \text{ mol dm}^{-3}$ (NaClO_4) at 40°C^a

[Hist]/ mol dm^{-3}	$k_{\text{obs}}/10^{-4} \text{ s}^{-1}$	
	pH = 5.20	pH = 8.04
0.03	0.77	9.80
0.05	1.14	14.89
0.07	1.55	19.35
0.10	2.11	27.85
0.15	3.07	41.20

^a $k_d = (1.93 \pm 0.10) \times 10^{-5} \text{ s}^{-1}$ at pH 5.20 and $(1.61 \pm 0.40) \times 10^{-4} \text{ s}^{-1}$ at pH 8.04.

**Fig. 1** A plot of k_{ox} vs. pH for the oxidation of histidine by $\text{Co}^{\text{III}}\text{W}$ with $[\text{Co}^{\text{III}}\text{W}] = 2.0 \times 10^{-4} \text{ mol dm}^{-3}$, $I = 1.0 \text{ mol dm}^{-3}$ (NaClO_4) and at 60°C 

Test for Free Radicals.—Both the reactions were tested for the generation of free radicals in the reaction mixture by the method reported earlier.⁶ The precipitation of a white polymer of acrylonitrile indicates that both the reactions proceed through the generation of free radicals. No polymerisation was encountered when the complexes and reagent were tested separately with acrylonitrile.

EPR Measurements.—Under the reaction conditions, the radicals were generated in a flow system, by mixing the complexes and reductant by volume in an EPR sample tube (flat cell) just outside the cavity of the spectrophotometer (E-4, Varian). The dissolved oxygen was then expelled by means of high vacuum pump, and the EPR tube was then placed in a Dewar. Conditions used were: temperature, 298 K ; scan range, 8000 G ; field set, 3000 G ; modulation amplitude, 12.5 G ; microwave frequency, 9.29 GHz ; time constant, 0.3 s ; scan time, 4 min . The radical generated in each oxidation of histidine by $\text{Co}^{\text{III}}\text{W}$ and $[\text{Mn}^{\text{III}}(\text{cdta})]^-$ gives a singlet with $g_c = 2.07$ and $g_{\text{Mn}} = 2.064$. The EPR measurements were also carried out at 77 K under the same conditions but in a mixture of methanol and DMSO. Here also a singlet at the same position as in aqueous solution was noted. The radical thus generated may be either $\text{RC}(\text{NH}_2)\text{COO}^-$ or $\text{RCH}(\text{NH}_2)\text{COO}^+$, but the product analysis definitely suggests the formation of radical $\text{RC}(\text{NH}_2)\text{COO}^-$ rather than $\text{RCH}(\text{NH}_2)\text{COO}^+$ in both reactions.

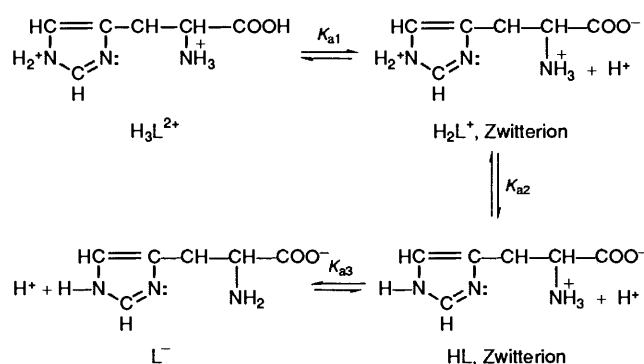
Results and Discussion

The redox reactions of histidine with $\text{Co}^{\text{III}}\text{W}$ and $[\text{Mn}^{\text{III}}(\text{cdta})]^-$ were investigated in the range pH 3.0–9.50 with variable concentrations of histidine and alkali cations at constant ionic strength and temperature. All the kinetic studies were carried out under pseudo-first-order conditions with excess of reagent (> 10 fold) over the oxidants. Typical spectral scanings at pH 4.0 for both the reactions gave no indication of inner-sphere complex formation between the reductant and oxidants. Plots of $-\log(A_t - A_\infty)$ vs. t (all the symbols have their usual significance) are all linear up to 90% of the total reaction indicating a first-order dependence of rate on both the oxidants. To get the dependence of rate on reductant, $[\text{Hist}]$ was varied at different pH for the two oxidants (Tables 1 and 2). A plot of k_{obs} vs. $[\text{Hist}]$ is a straight line passing through the origin for the reduction of $\text{Co}^{\text{III}}\text{W}$. But for the reduction of $[\text{Mn}^{\text{III}}(\text{cdta})]^-$, it gives a positive intercept on the rate axis. This indicates a first-order dependence of rate on reductant for both the reactions, and for the $[\text{Mn}^{\text{III}}(\text{cdta})]^-$ reaction the intercept manifests the occurrence of auto-decomposition of the complex. So the general rate expression for the oxidation of histidine with $\text{Co}^{\text{III}}\text{W}$ and $[\text{Mn}^{\text{III}}(\text{cdta})]^-$ can be given as eqn. (3) where k is

$$-d[\text{Ox}]/dt = 2k[\text{Ox}][\text{Hist}] \quad (3)$$

the electron transfer rate constant and 2 represents the stoichiometric factor.

The effect of acidity on the reduction of $\text{Co}^{\text{III}}\text{W}$ with histidine was investigated in the range pH 3.0–5.50 with $[\text{Hist}] = 0.03 \text{ mol dm}^{-3}$, $[\text{Co}^{\text{III}}\text{W}] = 2.0 \times 10^{-4} \text{ mol dm}^{-3}$, $I = 1.0 \text{ mol dm}^{-3}$ (NaClO_4) and temperature 60°C . The reaction rate increases with pH (Fig. 1) indicating the existence of protic equilibria of histidine. There are $\text{p}K_{a1}$, $\text{p}K_{a2}$ and $\text{p}K_{a3}$ for the stepwise removal of protons from the histidine dication (H_3L^{2+}) as shown below.



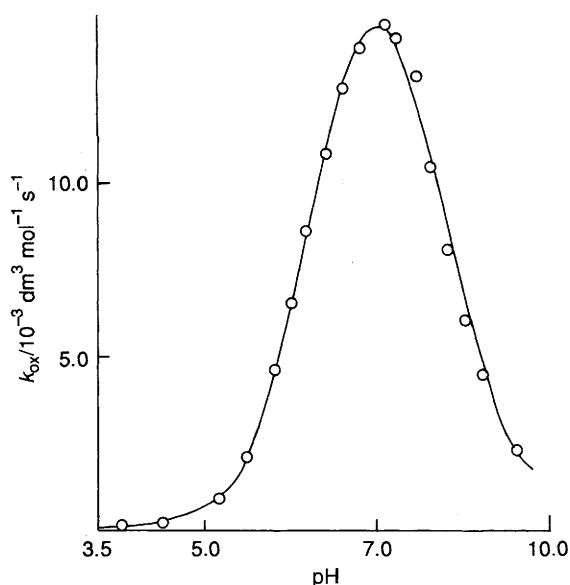
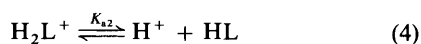


Fig. 2 A plot of k_{ox} vs. pH for the oxidation of histidine by $[Mn^{III}(cdta)]^-$ with $[Mn^{III}(cdta)]^- = 1.0 \times 10^{-3} \text{ mol dm}^{-3}$, $I = 0.50 \text{ (NaClO}_4\text{) mol dm}^{-3}$ and at 40°C . Solid line passes through the calculated values and the experimental values are shown by the points.

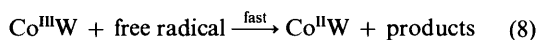
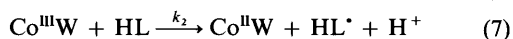
The carboxylic group has $K_{a1} = 1.70 \times 10^{-2} \text{ mol dm}^{-3}$, the imidazole nitrogen $K_{a2} = 8.32 \times 10^{-7} \text{ mol dm}^{-3}$ and the amino nitrogen $K_{a3} = 7.58 \times 10^{-10} \text{ mol dm}^{-3}$.⁷ Preliminary studies show that at high acidity ($\text{pH} < 1$) there is virtually no reaction and it may be concluded that H_3L^{2+} does not participate in the electron transfer process with $Co^{III}W$. This could also be true for the $[Mn^{III}(cdta)]^-$ reduction with histidine, though the latter is unstable below $\text{pH} 2.0$. For $Co^{III}W$ reduction, the predominant species in the experimental pH range are H_2L^+ and HL which are in equilibrium as shown in eqn. (4).



A plot of $k_{ox} (=k_{obs}/2[\text{Hist}])$ vs. $[H^+]^{-1}$ is a straight line with a positive intercept on the rate axis and this conforms to the rate equation (5). Considering the above observations and

$$k_{ox} = a + b[H^+]^{-1} \quad (5)$$

taking the stoichiometry as 2 the outer-sphere reaction scheme at constant $[Na^+]$ can be given as eqns. (6)–(8).



The theoretical rate expression corresponding to the above reaction scheme is given by eqns. (9) and (10). In the experi-

$$k_{obs} = 2 \frac{k_1[H^+] + k_2K_{a2}}{K_{a2} + [H^+]} [\text{Hist}] \quad (9)$$

$$k_{ox} = \frac{k_1[H^+] + k_2K_{a2}}{K_{a2} + [H^+]} \quad (10)$$

mental pH region $K_{a2} \ll [H^+]$ and eqn. (10) thus reduces to eqn. (11). Eqns. (5) and (11) are identical with $a = k_1$ and $b =$

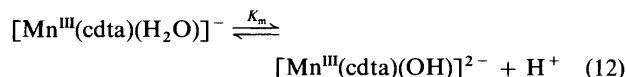
$$k_{ox} = k_1 + K_{a2}k_2[H^+]^{-1} \quad (11)$$

$K_{a2}k_2$. Experimental data have been fitted to eqn. (11) by means of a least-squares computer-fit program and the values of k_1 and $K_{a2}k_2$ are obtained from the intercept and slope respectively. Taking $K_{a2} = 8.32 \times 10^{-7} \text{ mol dm}^{-3}$, the values of rate parameters are calculated to be $k_1 = (8.36 \pm 2.28) \times 10^{-3} \text{ dm}^3 \text{ mol}^{-1} \text{ s}^{-1}$ and $k_2 = (1.45 \pm 0.02) \text{ dm}^3 \text{ mol}^{-1} \text{ s}^{-1}$.

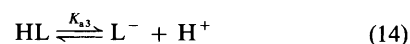
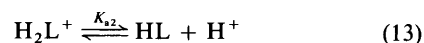
The dependence of rate on $[H^+]$ for the reduction of $[Mn^{III}(cdta)]^-$ with histidine was investigated in the range $\text{pH} 3.80\text{--}9.50$ with $[\text{Hist}] = 0.10 \text{ mol dm}^{-3}$, $[Mn^{III}(cdta)]^- = 1.0 \times 10^{-3} \text{ mol dm}^{-3}$, $I = 0.50 \text{ mol dm}^{-3}$ (NaClO_4) and temperature, 40°C and this seems to be quite interesting. A plot of $k_{ox} \{=(k_{obs} - k_d)/2[\text{Hist}]\}$, where k_d is the auto-decomposition rate of the complex (Table 2) vs. pH showed that the rate increases initially with pH, reaches a maximum around $\text{pH} 7.5$ and then decreases yielding a bell-shaped curve (Fig. 2).

The drop in rate with pH is associated with the deprotonation of the coordinated water molecule of $[Mn^{III}(cdta)(H_2O)]^-$ leaving $[Mn^{III}(cdta)(OH)]^{2-}$, which is unreactive towards the electron transfer process, and this can be explained by considering the fact that deprotonation of the oxidant results in a decrease in reduction potential.⁸ This observation has earlier been encountered in only a few reactions of $[Mn^{III}(cdta)]^-$.^{9–11}

The ionisation of $[Mn^{III}(cdta)(H_2O)]^-$ occurs as in eqn. (12).



The reported value of K_m is $7.76 \times 10^{-9} \text{ mol dm}^{-3}$.⁵ In the range $\text{pH} 3.8\text{--}9.5$ the existing reacting species of histidine are H_2L^+ , HL and L^- which are in equilibrium, as shown in eqns. (13) and (14). Taking $[Mn^{III}(cdta)(OH)]^{2-}$ as unreactive, the



outer-sphere reaction scheme for the oxidation of histidine with $[Mn^{III}(cdta)(H_2O)]^-$ can be depicted by eqns. (15)–(17). The resulting free-radicals react in a fast step to reduce another $[Mn^{III}(cdta)(H_2O)]^-$ ion to give the products, as in eqn. (18).

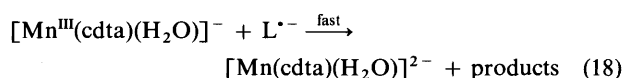
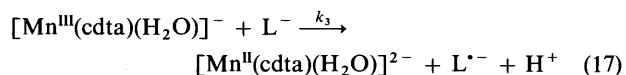
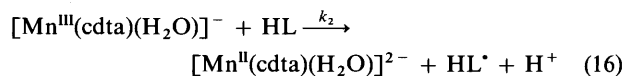
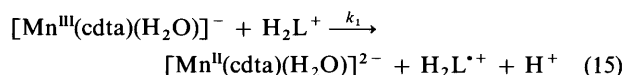


Table 3 Kinetic data for the variation of alkali-cation concentrations for the oxidation of histidine with $\text{Co}^{\text{III}}\text{W}$ and $[\text{Mn}^{\text{III}}(\text{cdta})]^-$

Oxidant	$[\text{M}^+]/\text{mol dm}^{-3}$	$k_{\text{obs}}/10^{-3} \text{ s}^{-1}$	
		Na^+	K^+
$\text{Co}^{\text{III}}\text{W}$	0.10	1.17	1.20
	0.30	1.25	1.44
	0.50	1.44	1.50
	0.70	1.52	1.69
	1.00	1.60	1.79
$[\text{Mn}^{\text{III}}(\text{cdta})]^-$	0.10	0.97	0.98
	0.50	0.97	0.99
	0.80	0.98	0.99
	1.00	0.98	0.99

^a $[\text{Co}^{\text{III}}\text{W}] = 2.0 \times 10^{-4} \text{ mol dm}^{-3}$, $[\text{Hist}] = 0.03 \text{ mol dm}^{-3}$, $\text{pH} = 4.0$ and at 60°C . $k_0 = (3.77 \pm 0.02) \times 10^{-2} \text{ dm}^3 \text{ mol}^{-1} \text{ s}^{-1}$ and $k_c = (1.68 \pm 0.02) \times 10^{-2} \text{ dm}^6 \text{ mol}^{-2} \text{ s}^{-1}$ for $[\text{Na}^+]$ variation and $k_0 = (3.97 \pm 0.02) \times 10^{-2} \text{ dm}^3 \text{ mol}^{-1} \text{ s}^{-1}$, $k_c = (2.14 \pm 0.03) \times 10^{-2} \text{ dm}^6 \text{ mol}^{-2} \text{ s}^{-1}$ for $[\text{K}^+]$ variation [using eqn. (20)]. ^b $[\text{Mn}^{\text{III}}(\text{cdta})]^- = 1.0 \times 10^{-3} \text{ mol dm}^{-3}$, $[\text{Hist}] = 0.03 \text{ mol dm}^{-3}$, $\text{pH} = 8.04$ and at 40°C .

Considering the protic equilibria for both the complex and reductant, and taking the stoichiometry as 2, the general rate expression corresponding to the above scheme is as in eqn. (19).

$$k_{\text{ox}} = \frac{k_1[\text{H}^+]^2 + k_2K_{a2}[\text{H}^+] + k_3K_{a2}K_{a3}}{[\text{H}^+]^2 + K_{a2}[\text{H}^+] + K_{a2}K_{a3}} \times \{[\text{H}^+]/(K_m + [\text{H}^+])\} \quad (19)$$

Eqn. (19) is solved by fitting the experimental data to it by means of a Simplex-optimisation programme and the best fit of data was obtained by allowing the values of K_{a2} , K_{a3} and K_m to be varied. The corresponding parameters evaluated are: $k_1 = (1.0 \pm 0.03) \times 10^{-4} \text{ dm}^3 \text{ mol}^{-1} \text{ s}^{-1}$, $k_2 = (1.79 \pm 0.05) \times 10^{-2} \text{ dm}^3 \text{ mol}^{-1} \text{ s}^{-1}$, $k_3 = (6.65 \pm 0.20) \times 10^{-2} \text{ dm}^3 \text{ mol}^{-1} \text{ s}^{-1}$ and $K_{a2} = (3.23 \pm 0.10) \times 10^{-7} \text{ mol dm}^{-3}$, $K_{a3} = (1.17 \pm 0.03) \times 10^{-9} \text{ mol dm}^{-3}$ and $K_m = (7.95 \pm 0.30) \times 10^{-9} \text{ mol dm}^{-3}$. The experimental and calculated k_{ox} values at different pH are in good agreement as shown in Fig. 2. The close agreement between the reported and kinetically determined values of proton equilibrium constants of histidine and $[\text{Mn}^{\text{III}}(\text{cdta})]^-$ strongly supports the proposed mechanism.

Effect of Alkali Metal Ions on the Reaction Rates.—An attempt was made to verify the effect of alkali-cation concentration, $[\text{M}^+]$ ($\text{M} = \text{Na}, \text{K}$) on the reaction rate for both reactions. For this purpose, keeping other conditions (pH , $[\text{Hist}]$ and temperature) constant, the concentration of alkali-cation added as supporting electrolyte was varied individually for both the reactions. For $\text{Co}^{\text{III}}\text{W}$ reduction, the rate increases with $[\text{M}^+]$ (Table 3) and a plot of k_{ox} vs. $[\text{M}^+]$ is a straight line with a common positive intercept on the axis for both cations. The rate equation, therefore, may be written as eqn. (20) where

$$k_{\text{ox}} = k_0 + k_c[\text{M}^+] \quad (20)$$

k_0 and k_c are the rate constants for the spontaneous and catalysed paths respectively (Table 3). To confirm whether this rate enhancement is due to specific cation catalysis or an ionic strength effect, experiments were carried out at constant $[\text{M}^+]$ but varying ionic strength, taking a mixture of salts like M_2SO_4 and MNO_3 . The results of this study once again demonstrate the importance of specific cation catalysis rather than the ionic strength effect.^{6,12,13} The cation catalytic order is $\text{K}^+ > \text{Na}^+$ and the difference is pronounced at relatively high pH. For

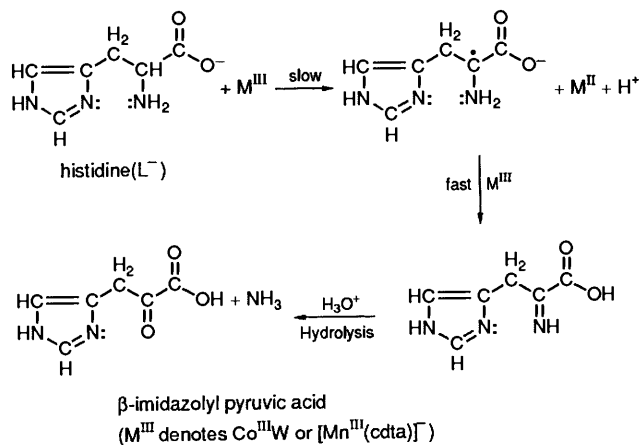
$[\text{Mn}^{\text{III}}(\text{cdta})]^-$ reduction, the rate enhancement with added M^+ is almost negligible (Table 3). This accounts for the smaller charge on the manganese(III) complex than the cobalt(III) species. The above order of alkali metal ion catalysis can be explained by considering the size of the hydrated cations which is in the order $\text{Na}^+ > \text{K}^+$. Thus K^+ would be more effective in outer sphere bridging between $\text{CoO}_4\text{W}_{12}\text{O}_{36}^{5-}$ and the reactive site on the histidine molecule *via* an ion-induced-dipole-type interaction.

It has been found that metal ions play a significant role in the enzymatic¹⁴ and non-enzymatic¹⁵⁻¹⁸ decarboxylation of histidine. Most of the enzymatic reactions have been duplicated by non-enzymatic model reactions in which pyridoxal or other appropriate aldehydes and suitable metals serve as catalysts.¹⁶ Only few recent reports have concerned the redox behaviour of histidine but there is a definite variation in the reactive site of the substrate, leading to different reaction products. In its oxidation by alkaline hexacyanoferrate(III),¹⁹ the reaction is believed to proceed through C-H bond fission on the α -carbon atom to give a keto-acid, β -imidazolyl pyruvic acid, as one of the reaction products. Similar studies on the redox interactions of histidine with electronically generated manganese(III)²⁰ and chloramine-T²¹ give aldehyde (RCHO) along with ammonia and carbon dioxide, instead of keto-acid, as the reaction products. In these reactions the carboxylate group of histidine was assumed to participate in the reaction. In our investigation, the oxidation products of histidine (β -imidazolyl pyruvic acid, NH_3) are the same as was noted in its oxidation by alkaline hexacyanoferrate(III).

Previous studies were confined to either highly acidic or alkaline conditions thereby evaluating the reactivity of only one reacting species of histidine. The present investigation, covering a wide range of pH, reflects the reactivity of the different reacting species of histidine available in the experimental pH region. A comparison of their reactivity showed that HL reacts 173 times faster than H_2L^+ for the oxidation of histidine by $\text{Co}^{\text{III}}\text{W}$. In the case of $[\text{Mn}^{\text{III}}(\text{cdta})]^-$ reduction, L^- reacts 3.7 times faster than HL which again reacts 179 times faster than H_2L^+ . Thus the general reactivity order is, $\text{H}_2\text{L}^+ < \text{HL} < \text{L}^-$. The large difference in reactivity between H_2L^+ and HL compared to that between HL and L^- can be explained by considering the following arguments: in H_2L^+ , both the protonated imidazole ring and $-\text{NH}_2$ group each exert a $-I$ effect and the availability of electron from the C-H bond is less. In HL, the deprotonated imidazole ring causes a $+I$ effect along with the $-I$ effect of the $-\text{NH}_3^+$ group. This combined effect probably causes greater availability of the electron leading to higher reactivity of HL. The $+I$ effect of the imidazole ring is operative both in HL and L^- , and the only difference is the absence of the $-I$ effect of NH_3^+ in L^- , which may be the cause of the small difference in reactivity between HL and L^- . The reactivity of a particular reacting species of histidine towards $\text{Co}^{\text{III}}\text{W}$ ($E^\circ = 1.0 \text{ V}$)²² and $[\text{Mn}^{\text{III}}(\text{cdta})]^-$ ($E^\circ = 0.81 \text{ V}$)⁵ is in accordance with their reduction potential values.

The lack of any spectral or kinetic evidence in favour of inner-sphere pathways leads us to propose an outer-sphere mechanism for the oxidation of histidine by both $\text{Co}^{\text{III}}\text{W}$ and $[\text{Mn}(\text{cdta})]^-$. The evidence of an outer-sphere mechanism for these oxidations of histidine by relating the difference in rate constants to the difference in reduction potential values of $\text{Co}^{\text{III}}\text{W}$ and $[\text{Mn}(\text{cdta})]^-$ requires that $\text{CoW}_{12}\text{O}_{40}^{6-5-}$,⁴ and $[\text{Mn}(\text{cdta})]^{2-/-}$ couples should have similar self-exchange rate constants and this is actually the case.

The evidence in favour of keto-acid product formation in the present oxidations of histidine leads us to conclude that C-H bond fission on the α -carbon atom is the most preferable pathway and the corresponding reactions are shown schematically below.



References

- 1 A. C. Andrews and E. W. Grundemeier, *J. Inorg. Nucl. Chem.*, 1966, **28**, 455.
- 2 R. J. Sundberg and R. B. Martin, *Chem. Rev.*, 1974, **74**, 471.
- 3 L. C. W. Baker and T. P. McCutcheon, *J. Am. Chem. Soc.*, 1956, **78**, 4503.
- 4 P. G. Rasmussen and C. H. Brubaker, *Inorg. Chem.*, 1964, **3**, 977.
- 5 R. E. Hamm and M. A. Suwyan, *Inorg. Chem.*, 1967, **6**, 139.
- 6 M. Ali, S. K. Saha and P. Banerjee, *J. Chem. Soc., Dalton Trans.*, 1990, 187.
- 7 L. G. Sillen, *Stability Constants of Metal Ion Complexes*, Special Publ., The Chemical Society, London, 1964, p. 506.
- 8 A. Chakravorty, *Comments Inorg. Chem.*, 1985, **4**, 1.
- 9 D. H. Macartney and D. W. Thompson, *Inorg. Chem.*, 1989, **28**, 2195.
- 10 I. K. Adzamlı, D. M. Davies, C. S. Stanley and A. G. Sykes, *J. Am. Chem. Soc.*, 1981, **103**, 5543.
- 11 S. Gangopadhyay, M. Ali, S. K. Saha and P. Banerjee, *J. Chem. Soc., Dalton Trans.*, 1991, 2729.
- 12 M. Ali, S. K. Saha and P. Banerjee, *Ind. J. Chem., Sect. A*, 1990, **29**, 528.
- 13 S. K. Saha, P. Bhattacharya, M. Ali and P. Banerjee, *Bull. Chem. Soc. Jpn.*, 1989, **62**, 3320.
- 14 P. Boyer, H. Lardy and K. Myrback, *The Enzymes*, 2nd edn., Academic Press, New York, 1960, vol. 2, p. 115.
- 15 B. Guirard and E. Snell, *J. Am. Chem. Soc.*, 1954, **76**, 4745.
- 16 D. E. Metzler, M. Ikawa and E. E. Snell, *J. Am. Chem. Soc.*, 1954, **76**, 648.
- 17 E. Werle and W. Koch, *Biochem. Z.*, 1949, **319**, 305.
- 18 A. Goudot, *C. R. Hebd. Seances Acad. Sci.*, 1955, **240**, 975.
- 19 D. Laloo and M. K. Mahanti, *J. Chem. Soc., Dalton Trans.*, 1990, 311.
- 20 Ivan Pinto, B. S. Sherigara and H. V. K. Udupa, *Bull. Chem. Soc. Jpn.*, 1990, **63**, 3625.
- 21 T. Gowda and R. V. Rao, *Ind. J. Chem., Sect. A*, 1986, **25**, 908.
- 22 L. Ebersson, *J. Am. Chem. Soc.*, 1983, **105**, 3192.

Paper 2/00091A

Received 8th January 1992

Accepted 13th February 1992